Journal of Polymers and the Environment
https://doi.org/10.1007/s10924-019-01428-9

ORIGINAL PAPER

Study on Mechanical and Thermal Properties of Poly(Lactic acid)/Poly(Butylene adipate-co-terephthalate)/Office Wastepaper Fiber Biodegradable Composites

Chong Xu[1] · Xiaolin Zhang[1] · Xiao Jin[1] · Sunjian Nie[1] · Rui Yang[1]

Abstract
Office wastepaper fibers(OWF)/poly(butylene adipate-co-terephthalate) (PBAT)/poly(lactic acid) (PLA) biodegradable composites with different mass ratio were made by melt blending and injection moulding process. At the same time, the use of MAPLA and KH560 was studied as a potential approach for improving interfacial adhesion between OWF, PBAT and PLA. The results revealed that with the increasing of PBAT, the notched impact strength of PLA/PBAT/OWF composites can be first increased and then decreased. When the content of PBAT was 20 wt%, the notch impact strength of PLA/PBAT/OWF composite was the highest, increased by 291% compared with pure PLA. TGA results revealed that the onset degradation temperature of the composites can be increased and its thermal decomposition step can be changed. According to the crystallization and melting performance table, OWF can act as nucleating agent to promote the crystallization properties of composites, while PBAT can prevent the crystallization and the higher the content is, the more obvious it is. It can be seen from the SEM figures that the addition of MAPLA and KH560 simultaneously makes the composites interface bond closer, thus improving the interface performance of PLA/20PBAT/OWF composite. Among the three kinds of modified composites, PLA/20PBAT/OWF/MK composite has the lowest water absorption and the best comprehensive performance.

Keywords Biocomposite · Mechanical properties · Thermal properties · Interface modification

Introduction

Along with the development of people's living standard, the increasing demand for oil resources and the strengthening of environmental protection, the utilization of renewable resources to replace non-renewable resources is becoming increasingly important [1, 2]. Green composites are a combination of natural fibers and bioplastics. Due to its biodegradability, low density and reproducibility, it has become a promising alternative to traditional synthetic materials and petroleum-based composites [3]. Therefore, more and more experts and scholars have paid attention to the preparation of biodegradable composites by using bioplastics, natural fibers or regenerated fibers and other sustainable and environment-friendly materials [4, 5].

Poly (lactic acid) (PLA), also known as poly (lactide), which is a linear aliphatic thermoplastic polyester, is a biodegradable polymer prepared from corn and other starch plants by fermentation and polymerization with good biocompatibility, mechanical properties and processability [6–8]. However, the wide application of polylactic acid is limited to a certain extent because of the limitations of its molecular chain structure, such as slow crystallization, high brittleness, poor hydrophilicity and heat resistance [9, 10]. Therefore, it is particularly important to improve its heat resistance and toughness. Joffre et al. [11] prepared 100% renewable composite materials by using acetylated wood fiber as filler and polylactic acid as matrix. The results showed that the effects of acetylation on the adhesion between wood fiber and polylactic acid group were different under different water content. When the crack of the composite increases, the interface of the fiber and matrix can still transfer the load (redistribution stress), thus improving the toughness and strength of the material. At present, the application of

✉ Xiaolin Zhang
zxlbmm@sina.com

[1] Faculty of Printing, Packing Engineering and Digital Media Technology, Xi'an University of Technology, Xi'an 710048, People's Republic of China

Published online: 27 March 2019

PLA materials has been developed from the early packaging, medical materials and other short-cycle commodities to daily necessities, agriculture, forestry, aquatic products and other long-life cycle commodities and even in the fields of automobile, electronics, construction and so on [12–14].

Poly(butylene adipate-co-terephthalate) (PBAT) is an aliphatic aromatic copolyester that can be completely biodegradable [15]. Unlike PLA, PBAT is a flexible elastomer with low strength and high elongation at break($\geq$600%). In addition, PBAT is known as a good toughening material for PLA because of its biodegradability and high toughness [16]. PBAT/PLA composites were investigated by Urquijo et al. [17]. In order to toughen PLA, PBAT was used as matrix to prepare PBAT/PLA composites by melt blending method. The notched impact strength of composites was measured. The results demonstrated that the notched impact strength of PBAT/PLA composites in the case of the 40/60 composition was higher than 100 J/m, which was much higher than that of pure PLA. At present, PBAT is mostly used in agricultural plastic film or environmental protection garbage bag, but the degradation rate of PBAT is slow due to the existence of aromatic chain [18].

The waste of more and more paper resources has aroused widespread concern in various countries, including office waste paper [19]. It is reported that recycling a ton of waste-paper can save about 3–4 m^3 wood, 1.2 t coal, 600 kW h electricity and 100 t water, and reduce the consumption of forest resources and the discharge of toxic waste, which has tremendous economic and environmental benefits [20]. As a result, how to rationalize the utilization of waste paper has become a task of environmental protection significance. Waste paper fiber mainly comes from all kinds of paper products and contains a lot of cellulose, which is similar to natural plant fiber [21]. Many researchers use waste paper fibers to strengthen polyolefin materials, and the mechanical properties of composites is significantly increased. Zhang et al. [22] prepared composites with two different waste paper fibers reinforced with waste PP, and used 2 wt% MAPP as coupling agent. The results demonstrated that the mechanical properties of WPF(waste paper fibers)/PP composites were the best at 30 wt% content of waste paper fiber.

Although recycling of waste paper has attracted attention, its development research is not extensive [23]. Some possible reasons include limited compatibility between the waste paper fiber and the matrix and poor dispersion of waste paper fiber in the thermoplastic melt, which leads to unsatisfactory final performance of the composites [24]. The research results of Qian et al. [25] showed that the mechanical properties of composites were closely related to the properties of matrix, nature of fillers and interfaces between matrix and fillers. The major defects of composites with fiber are poor interfacial adhesion and the low compatibility between the hydrophobic matrix polymer and the hydrophilic fiber filler. Therefore, it is of great significance to investigate the interfacial bonding between regenerated fiber fillers and biodegradable polymers matrix [8]. Various studies improving the interfacial properties of PLA/natural fiber composites (binary composites) by chemical and physical treatment of natural fibers and the addition of grafted polymer have been performed [26, 27]. However, there are few studies on the application of these modification methods in PLA-based ternary composites.

The aim of this paper is to investigate the mechanical properties, crystallization properties, thermal properties and water absorption of PLA/PBAT/OWF composites with different PBAT contents. At the same time, considering the interfacial bonding, the effects of different modification methods on the crystallization properties and mechanical properties of PLA/20PBAT/OWF composites (ternary composites) were studied.

Experimental

Materials

Poly(lactic acid) (PLA) (Nature Works 3052D, Mw = 140,000, 96% of L-lactide) was supplied by Nature Works Co. Ltd. PBAT (Tm = 115 °C, density 1.25–1.28 g/cm^3, Ecoflex F Blend C1200) was purchased from BASF Company. OWF was collected from our laboratory. The collected wastepaper was shredded into 20 mm × 10 mm pieces by paper shredder and smashed with a high speed pulverizer for 50–60 s to obtain office wastepaper fibers. The average length and width of the recycled office waste-paper fibers were 950 μm and 30 μm respectively. Anhydrous ethanol was obtained from Shandong Baiqian Chemical Co. Ltd., China. The silane coupling agent KH560 was supplied by Nanjing Chuangshi Chemical Additives Co. Ltd., China. MAPLA, commercial grade, was purchased from Dongguan Shengbang Engineering Plastics Material Co. Ltd., China.

Pretreatment of Wastepaper Fiber

Firstly, OWF was dried in an electric oven at 70 °C for 12 h. Then KH560 was put into the solution of *W*ethanol/*W*water = 90/10 and stirred for 10 min for hydrolysis. Subsequently, the OWF was immersed in 2 wt% of KH560 solution in the thermostat water bath at 50 °C for 3 h and stirred every 10 min. Finally, the OWF was dried in an electric oven at 70 °C for 12 h to obtain KH560 modified office wastepaper fiber (KOWF).

Preparation of PLA/PBAT/OWF Composites

Firstly, PLA, PBAT and OWF were dried under vacuum at 70 °C for 8 h. Then they were mixed by a two-roll plastic mill at 160 °C and 10 rpm for 6–8 min. Afterwards, PLA/PBAT/OWF blends were smashed with the high-speed universal pulverizer and dried under vacuum at 70 °C for 5 h. Finally, PLA/PBAT/OWF particles were processed by an injection Molding Machine (TA AI MACHINERY, China) for standard specimen. The PLA/PBAT/OWF/2 M, PLA/PBAT/OWF/2 K and PLA/PBAT/OWF/MK composites were prepared by the above process similarly, the difference was that the PLA, PBAT and OWF were mixed by adding different interface modifying agent with 2 wt% MAPLA, 2 wt%KH560 or 2 wt% MAPLA and 2 wt%KH560. The prescriptions of composites were shown in Table 1.

Characterization

Fourier Transform Infrared Spectroscopy (FTIR)

The virgin OWF and KOWF were analyzed by FTIR spectrometer (FTIR-8400S, Shimadzu, Japan). The samples were entirely dried in an electric oven before prepared as KBr pellet. The FTIR spectroscopy was performed in the wave number ranging from 4000 to 400 cm^{-1}. Forty scans were co-added.

X-ray Diffraction (XRD)

The crystalline structures of different OWF samples were investigated by an x-ray diffractometer (Bruker D8 ADVANCE). A scanning of 2θ angles of 10°–30° was performed with the scan speed of 8.0000°/min, and the machine was operated at 40 kV and 35 mA.

Mechanical Properties

According to GB/T 1447-2005 standard, the tensile properties of the PLA/PBAT/OWF composites were measured using a XWW-20A Electronic Universal Testing Machine (Shanghai standard instrument equipment Co. Ltd., China) at a tensile speed of 5 mm/min. All dumbbell shaped samples with a size of 120 mm length, 10 mm width, and 4 mm thickness were studied.

The flexural properties of the composites were carried out under in a XWW-20A Electronic Universal Testing Machine (Shanghai standard instrument equipment Co. Ltd., China) in accordance with GB/T 1449-2005 at a span of 64 mm and a speed of 2 mm/min. The dimension of each flexural testing sample was 85 mm × 10 mm × 4 mm.

According to GB/T 1043.1-2008, the notch impact strength of the composites was measured in a YF-8109 test machine (Yangzhou Yuanfeng testing machine Ltd., China) according to GB/T 1043.1-2008. The specimen with the size of 80 mm × 10 mm × 4 mm was carved a standard V-notch with a depth of 2 mm.

All measurements were performed at 20 °C. The values of mechanical properties of each group samples were obtained by six tests.

Thermogravimetric Analysis (TGA)

TGA was carried out under nitrogen atmosphere with a thermogravimetric analyzer (NETZSCH STA 449 F3). The samples weighing about 8 mg were taken in an alumina crucible and heated from 30 to 600 °C with heating rates of 20 °C/min and a nitrogen flow of 20 ml/min.

Differential Scanning Calorimetry (DSC)

Thermal properties of the composites were investigated under nitrogen atmosphere with NETZSCH DSC 200 F3 machine to acquire thermograms of composites. Specimens weight was about 5–8 mg and the heating rate was 15 °C/min. DSC was carried out twice to eliminate the influence of thermal history on composites, and the specimens were heated from 20 to 200 °C.

Table 1 Prescriptions of the composites

Materials	PLA (wt%)	PBAT (wt%)	OWF (wt%)	MAPLA (wt%)	KH560 (wt%)
PLA/10PBAT/OWF	80	10	10	–	–
PLA/20PBAT/OWF	70	20	10	–	–
PLA/30PBAT/OWF	60	30	10	–	–
PLA/40PBAT/OWF	50	40	10	–	–
PLA/20PBAT/OWF/2M	68	20	10	2	–
PLA/20PBAT/OWF/2K	68	20	10	–	2
PLA/20PBAT/OWF/MK	66	20	10	2	2

Scanning Electron Microscopy (SEM)

The surface morphology of tensile fractured surfaces of composites was observed and analyzed by SEM (SU 8000, Hitachi Limited, Japan) working at accelerating voltage of 2.0 kV in the vacuum mode. Before measurement all specimens were sputtered with gold using a vacuum sputter coater for 60 s at argon pressure of 10 Pa and current of 40 mA.

Water Absorption Performance

The water absorption of composites was tested according to GB/T1462-2005 in which the samples were immersed in water for 24, 48, 72, 96, 120, 144 and 168 h at room temperature. The weight gain of composites was recorded daily on a high precision balance after taking out specimens and wiping them with a facial tissue. The water absorption percentage of composites was calculated as follows:

$$\mathrm{WA}(\%) = \frac{m_1 - m_0}{m_0} \times 100 \quad (1)$$

where WA is the water absorption percentage, m_0 is the initial dry weight of the PLA/PBAT/OWF composites and m_1 is the weight of the PLA/PBAT/OWF composites after immersion.

Results and Discussion

FTIR Analysis

The FTIR spectroscopy of original and silane coupling agent-treated OWF were shown in Fig. 1. The FTIR spectrum of OWF (curve-a) was basically identical with the representative absorptions of vegetable fiber. The spectra of OWF and KOWF had a broad and strong band from 3600 to 3100 cm^{-1}, which represented the free O–H stretching vibration in plant fiber [22]. After treatment with KH560, the free O–H stretching vibration peak at 3347 cm^{-1} was significantly weakened, which was caused by the reaction of KH560 with hydroxyl groups in OWF. The results of OWF and KOWF spectra demonstrated that hemicellulose has the characteristic of C-H stretching vibration near 2903 cm^{-1}. The bending vibration peak at 1635 cm^{-1} that was weakened to some extent after KH560 modification was related to the adsorption of water by plant fibers, which further indicated that the absorbability of composites was reduced. Besides, the three peaks demonstrated in the FTIR spectrum of OWF at 1058 cm^{-1}, 1112 cm^{-1} and 1163 cm^{-1} were connected with the C–O–C stretching vibration, the C–O–C glycosidic ether band and the C–C ring breathing band [21]. The Si–O–C stretching vibration peak was not found in the FTIR spectrum of KOWF, which may be caused by C–O–C glycosidic ether band at 1112 cm^{-1} covering this peak. Furthermore, the three peaks around 1427 cm^{-1}, 874 cm^{-1} and 712 cm^{-1} were related to carbonate inorganic complex, which may be caused by the printing ink in OWF and KOWF [30–32].

XRD Analysis

The crystalline structure of the virgin OWF and KOWF were determined by X-ray diffraction. The diffraction peaks presenting around 16.3° and 22.6° in Fig. 2 were attributed to the 101 and 002 characteristics crystal planes in cellulose I respectively [21]. The lowest trough diffraction intensity occurs near 2θ = 18°, which is the scattering intensity of diffraction in the amorphous region of the fiber, while the intensity of highest diffraction peak at 2θ = 22.6° was used to evaluate the

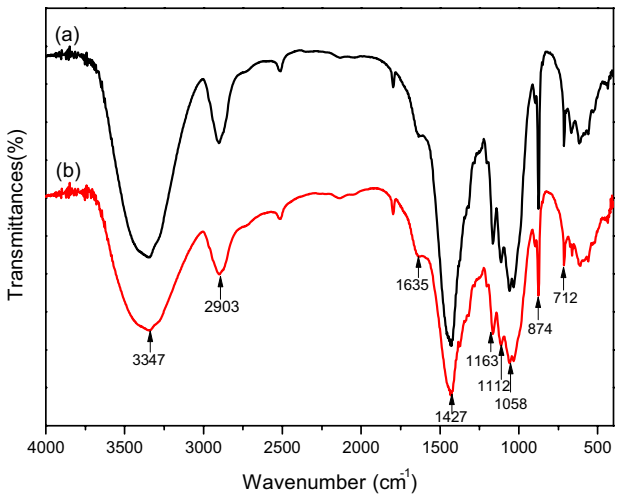

Fig. 1 FTIR spectra of **a** OWF and **b** KOWF

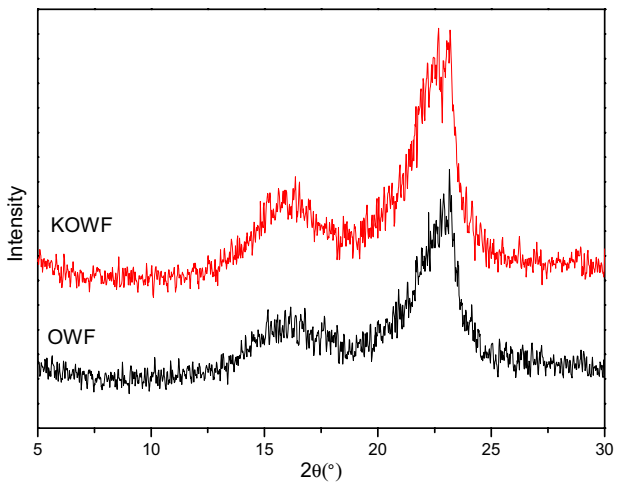

Fig. 2 XRD graphs of OWF and KOWF

crystallinity index (CI). After KH560 treatment, the position of the diffraction peak of cellulose did not change, but the diffraction intensity of the 002 lattice planes peak of cellulose increased obviously. This result suggested that KH560 treatment did not change the crystalline form of cellulose.

The degree of crystallinity was obtained from crystallinity index (CrI) calculated by the following formula:

$$CrI(\%) = \frac{I_{002} - I_{am}}{I_{002}} \times 100 \quad (2)$$

where I_{am} is the scattering intensity of amorphous cellulose which is adopted the lowest peak at about 18° and I_{002} is the diffraction intensity of the 002 crystalline peak of cellulose at around 22.6° [28]. Table 2 listed changes of *CrI*. Results showed that *CrI* of KOWF cellulose was slightly higher than OWF, which made clear that KH560 treatment had little effect on crystallinity of OWF cellulose.

Table 2 Crystallinity index of OWF and KOWF

Samples	101(°)	002(°)	Crystalline index (*CrI*) (%)
OWF	16.3	22.6	67.5
KOWF	16.4	22.6	68.3

Mechanical Properties

Figure 3a demonstrated the tensile strength and notched impact strength of neat PLA and PLA/PBAT/OWF composites. As the increase of PBAT content, the tensile strength of composites was reduced stepwise, which was due to the fact that PBAT is an elastic polymer and its tensile strength is low [16]. The existence of waste paper fiber can increase the interfacial compatibility of PBAT and PLA, but the content of PBAT increases gradually, the stress load of waste paper fiber cannot provide enough support to maintain the tensile strength of the composites. Besides, when the content of PBAT increased gradually, it was easier to occur phase separation PBAT and PLA, and the waste paper fiber was easier to agglomerate at the interface. As the increasing PBAT content, the impact strength of the composites firstly improved

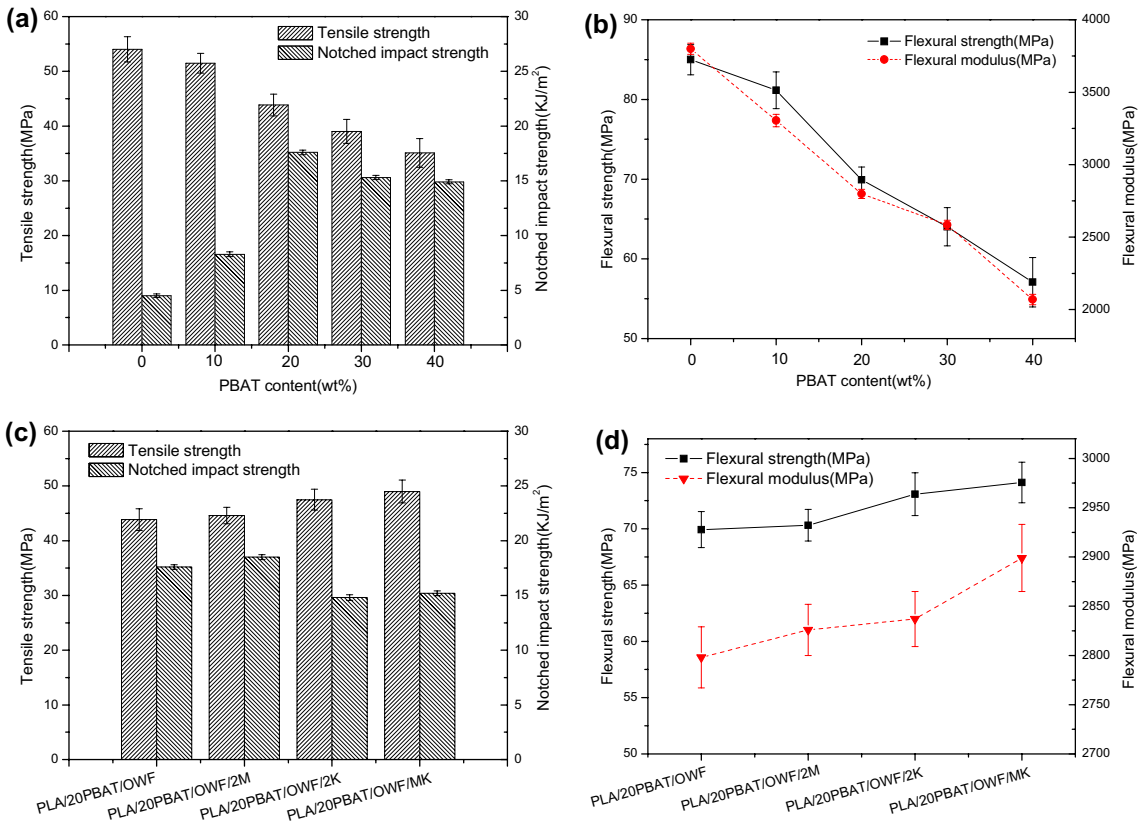

Fig. 3 **a** The tensile and notched impact strength of pure PLA and PLA/PBAT/OWF composites with different PBAT content; **b** the flexural strength and modulus for neat PLA, PLA/PBAT/OWF composites with different PBAT content; **c** the tensile and notched impact strength of composites adding different interfacial modifiers; **d** the flexural strength and modulus of composites adding different interfacial modifiers

and then reduced. At 20 wt% content of PBAT, the notched impact strength of composites was the highest (17.6 kJ/m^2), increased by 291% compared with pure PLA (4.5 kJ/m^2). Because PBAT is an elastomer polymer with high toughness and high impact strength, adding it to the PLA matrix can increase the toughness of composites. At the same time, the addition of waste paper fiber can effectively bond to the interface between PLA and PBAT. It can better provide the stress load for the composites. When the content of PBAT is too high, the interface between PLA, PBAT and waste paper becomes blurred, and the stress cannot be transferred effectively, which leads to the decrease of impact strength.

The flexural strength and flexural modulus for neat PLA, PLA/PBAT/OWF composites were presented in Fig. 3b. The flexural strength and modulus of the composites decreased slowly when the amount of PBAT was varied from 10 to 40 wt%, which were consistent with the tensile test results. At PBAT content 20 wt%, the flexural strength and flexural modulus were 69.93 MPa and 2798 MPa, which were decreased by 17.8% and 26.4%, respectively, as compared with pure PLA. As PBAT is an elastomer polyester, with the increase of its content, the composites become softer, bringing on the reduction of flexural strength and flexural modulus.

Adding interfacial modifier in composites is an effective method to improve interfacial properties between matrix and fiber, which is also the hot spot of current research. The tensile strength and notched impact strength of the composites adding different interfacial modifiers were presented in Fig. 3c. Compared with the unmodified composites, the tensile strength of the composites with adding 2 wt% MAPLA and 2 wt%KH560 alone were increased slightly, and the tensile strength of the composites adding 2 wt% MAPLA and 2 wt% KH560 in combination was up to 48.97 MPa, which was higher than that of the unmodified composites by 11.7%. This is due to the uniform distribution of interfacial modifiers in the composites and the formation of a bridge between matrix and fiber, which improves the interfacial properties of the composites. The impact strength of PLA/20PBAT/OWF adding 2 wt% MAPLA is the optimal, increased by 5.1%, the impact strength of PLA/20PBAT/OWF adding 2%KH560 is the lowest, reduced by 15.9%, and the impact strength of PLA/20PBAT/OWF adding 2MAPLA and 2KH560 is the middle, reduced by 13.6%, respectively, as compared with PLA/20PBAT/OWF. But all the impact strength of three samples were much higher than pure PLA. Since MAPLA is softer than pure PLA, which enhances the toughness of composites, and the toughness of MAPLA itself is greater than as interfacial modifier, which leads to the increase of impact strength. KH560 can make the interface bonding more closely, which leads to the reduction of impact strength. The present of two kind of interfacial modifiers has a more compact interface than the only present of MAPLA, which makes the impact strength of the composite higher than that of the composites with only present of KH560, but is lower than that of the unmodified composite.

The effect of adding different interfacial modifiers on the flexural strength and modulus of the composites were presented in Fig. 3d. The flexural strength and modulus of the three kinds of modifiers composites gradually increased and had significant improvements compared with composites without modification, which was consistent with the results of tensile tests. Compared with the unmodified composite, the flexural strength and modulus of the compound modified composites was the highest, increased by 6% and 3.6%, respectively. Because between the fiber and the matrix, the matrix and the matrix were bonded more closely by adding KH560 and MAPLA, and the interfacial properties of the composites were increased.

TG Analysis

The effect of thermostability of PLA/PBAT/OWF composites with different PBAT content was valued by thermogravimetry. Figure 4 demonstrated the thermograms of PLA/PBAT/OWF composites with different PBAT content. The curve of DTG was shown in Fig. 5, and Table 3 tabulated the thermal degradation data. It was found that pure PLA started decomposing at 288 °C(T_{oneset}) and just 0.1% was left at 600 °C. The initial decomposition temperature of the composites was improved significantly with the addition of PBAT and OWF. However, some researchers analyzed the thermostability of PLA/Ramie composites, and concluded that the addition of ramie fiber could reduce the initial decomposition temperature of the composites [18]. This is contrary to the experimental results, which may be due to the addition of PBAT to improve the thermostability

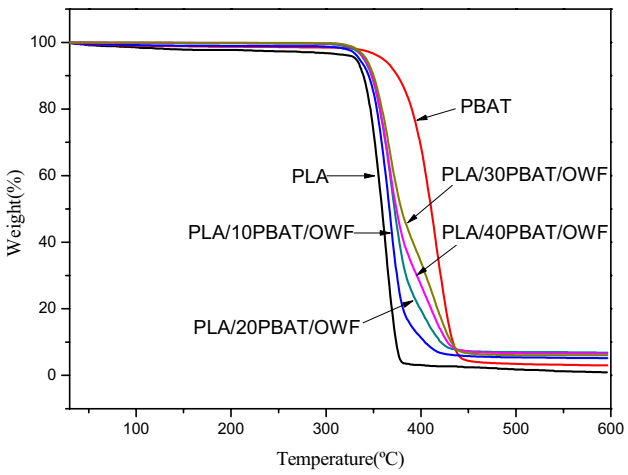

Fig. 4 TGA curves of neat PLA, PBAT and PLA/PBAT/OWF with different PBAT content

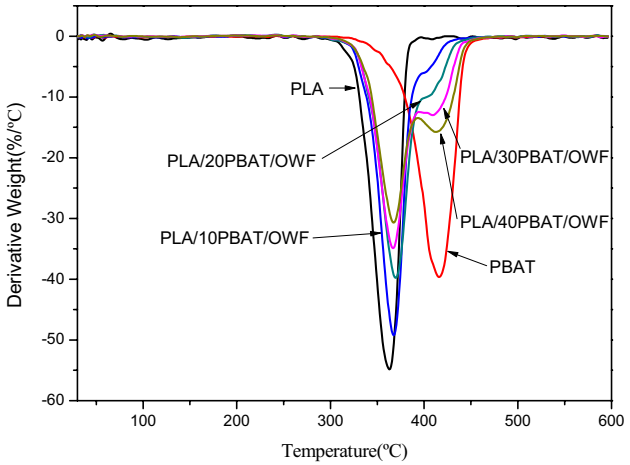

Fig. 5 DTG curves of neat PLA, PBAT and PLA/PBAT/OWF with different PBAT content

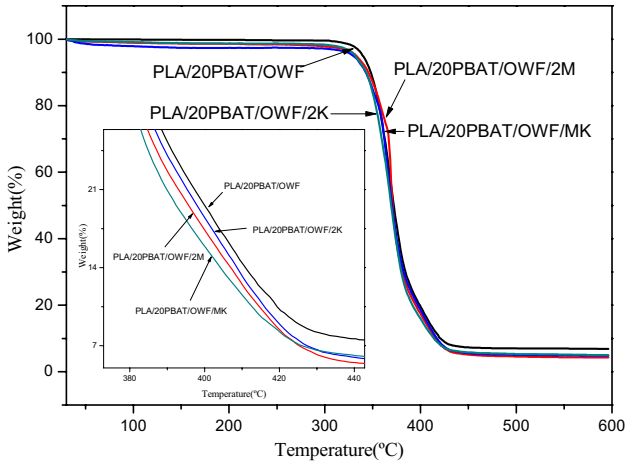

Fig. 6 TGA curves of PLA/20PBAT/OWF without and with different interfacial modifiers

of the composites. As the increase of PBAT content, the initial decomposition temperature, termination temperature and T_{max} increased gradually, which indicated that the thermal stability of the composites was gradually improved. From the DTG diagram, we could see that the composite had two steps of decomposition, the first step was the decomposition of PLA/OWF composite, the second step was the decomposition of PBAT.

Figure 6 showed the effect of different interfacial modifiers on the thermogravimetric curves of composites, and the DTG curves were presented in Fig. 7. The correlation characteristic curve was shown in Table 3. The results revealed that the thermal stability of composites with modifier was nearly the same as that of untreated composites. It could be seen from the table that the decomposition of the first step PLA/OWF composite was near 368 °C, indicating that the interfacial modifier had no significant effect on the thermal stability of PLA/OWF, while the decomposition of the second part of PBAT was near 406 °C, indicating that the modifier had no significant effect on the thermal stability of PBAT. At 600 °C, the coke residue of pure PLA was 1%, which was obviously lower than that of PLA/PBAT/OWF composites in same condition, which indicated that the existence of OWF and PBAT reinforced the carbonization process of the composites.

DSC Analysis

Figure 8 presented the DSC quadratic heating curve of PLA/PBAT/OWF composites with different mass ratios. The glass transition temperature (T_g), crystallization temperature (T_c), crystallization enthalpy (ΔH_c), melting enthalpy (ΔH_m), melting temperature (T_m) and crystallinity (X_c) acquired from the DSC researches were listed in Table 4. The secondary heating curve of pure PLA had a cold crystallization peak, which was due to the high rigidity of the PLA molecular chain and was not easy to be fully arranged in the process of cooling crystallization. The segment of the

Table 3 TG characterization of the samples

Samples	T_{onset} (°C)	T_{50} (°C)	T_{max} (°C)		$T_{residues}$ (°C)	Residue (%) (600 °C)
PLA	288	358	363		394	1
PBAT	320	411		416	472	3
PLA/10PBAT/OWF	295	366	367	402	449	5.2
PLA/20PBAT/OWF	300	372	369	406	455	6.8
PLA/30PBAT/OWF	304	374	366	409	473	6.6
PLA/40PBAT/OWF	306	379	367	412	474	6
PLA/20PBAT/OWF/2M	300	371	368	407	455	4.3
PLA/20PBAT/OWF/2K	299	370	368	406	455	4.8
PLA/20PBAT/OWF/MK	298	369	369	406	455	5

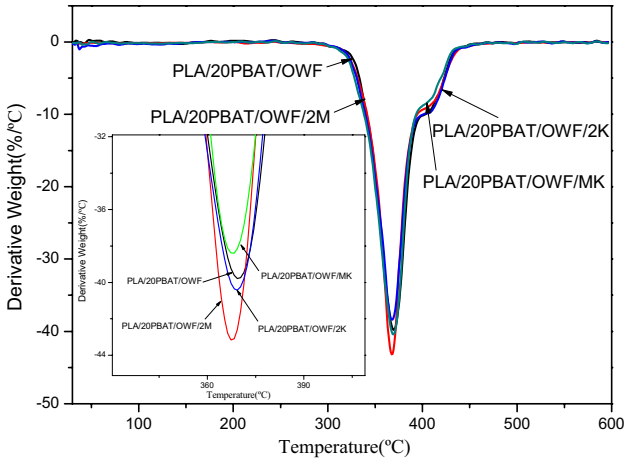

Fig. 7 DTG curves of PLA/20PBAT/OWF without and with different interfacial modifiers

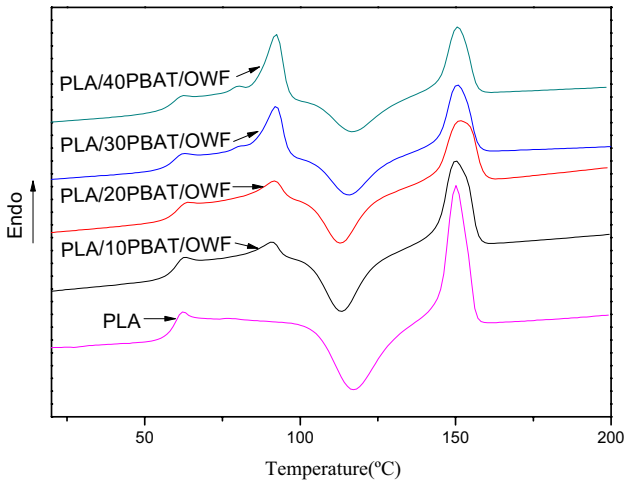

Fig. 8 DSC thermograms of neat PLA and PLA/PBAT/OWF with different PBAT content

molecular chain which had no time to crystallize would absorb the energy to form an ordered structure in the process of heating up again. As the increase of PBAT content in composites, the T_g of PLA did not change obviously, and remained at around 62 °C. Adding OWF and PBAT at the same time lead to the T_c of PLA in the composite decreased from 116.3 °C to 113.1 °C, whilst T_g did not change obviously. As the increasing of PBAT, T_c of PLA in the composite gradually increased from 113.1 °C to 117.1 °C, indicating that OWF and PBAT promoted the transfer of PLA chain in PLA system and played a role in nucleation. However, with the increasing of PBAT, the molecular chain movement and cold crystallization of PLA would be blocked.

The crystallinity (X_c) values of PLA in the PLA/PBAT/OWF composites were calculated by the following formula:

$$X_c(\%) = \frac{\Delta H_m}{\emptyset \Delta H_m^0} \times 100 \quad (3)$$

where ΔH_m is the melting enthalpy for PLA, Φ is the weight fraction of PLA in the PLA/PBAT/OWF composites and ΔH_m^0 is the theoretical enthalpy of 93.7 J/g for thoroughly crystalline PLA [15]. As the increase of PBAT content in composites, the T_m of PLA in the composite first increased and then declined, but change was not significant in overall, while the crystallinity of PLA decreased gradually. This could be related to the addition of PABT. With the increasing of PBAT, the regularity of the molecular chain is further reduced, resulting in the gradual decrease of the crystallinity of the composites.

Figure 9 showed the effect of adding diverse modifiers on the crystalline properties of composites. Detailed data were shown in Table 4. It could be seen from the quadratic heating figure of PLA/20PBAT/OWF/MK composite that two melting peaks appeared in PLA, the low temperature peak weakens and the high temperature peak increased. The double melting behavior could be explained according to the theory of melt recrystallization. The low temperature peak was the melting of the crystalline component formed in the cold crystallization process, while the high temperature peak was the addition of recrystallization melting result. The addition of KH560 caused the cold crystallization peak to shift to the high temperature direction. The crystallinity increased slightly. This was due to the fact that the coupling agent made the interface more tightly bound, hinders the

Table 4 Crystallization and melting properties of the samples

Samples	T_g (°C)	T_c (°C)	ΔH_c (J/g)	ΔH_m (J/g)	T_{m1} (°C)	T_{m2} (°C)	T_{m3} (°C)	X_c (%)
PLA	62.4	116.9	−16.22	20.58		150.1		21.9
PLA/10PBAT/OWF	62.9	113.1	−12.67	18.48	91.1	150.4		24.6
PLA/20PBAT/OWF	62.8	113.3	−11.58	15.86	91.7	151.3		24.1
PLA/30PBAT/OWF	62.9	115.6	−9.78	13.41	92.1	150.7		23.8
PLA/40PBAT/OWF	62.4	117.1	−8.76	11.09	92.3	150.7		23.6
PLA/20PBAT/OWF/2M	62.9	110.1	−14.42	18.26	91.1	149.3	154.3	27.8
PLA/20PBAT/OWF/2K	62.5	115.2	−12.22	16.33	91.2	150.2		24.8
PLA/20PBAT/OWF/MK	62.5	108.2	−11.79	16.84	91.1	148.8	154.9	25.6

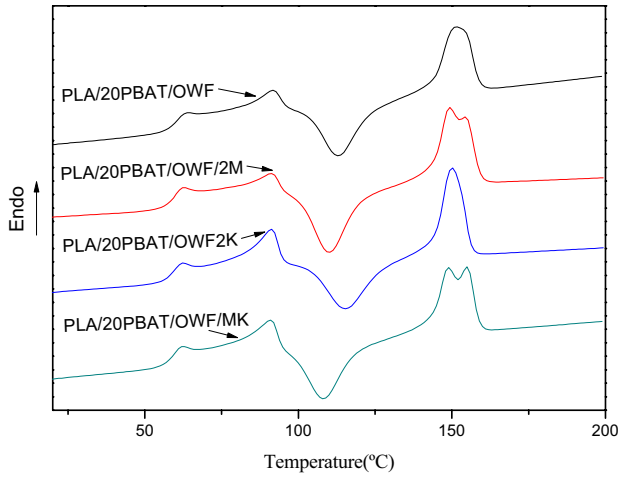

Fig. 9 DSC thermograms of PLA/20PBAT/OWF without and with different interfacial modifiers

movement of PLA molecular chains to some extent, and impedes the cold crystallization of PLA. The addition of MAPLA served as a nucleating agent, and the PLA molecular chain could start to crystal growth and heterogeneous nucleation with MAPLA as the core at lower temperature. The addition of a small amount of MAPLA could obviously improve the nucleation effect of heterogeneous phase and increased the crystallinity of PLA in composites.

SEM Analysis

In order to study the compatibility between PLA, PBAT and OWF, the morphology of fracture surface of tensile specimen was observed by SEM. Figure 10a–e demonstrated the morphology of the five samples. With the addition of PBAT and OWF in Fig. 10a, the voids of the composites increased and the interfacial bonding became loose, which resulted in the decrease of the tensile strength and bending strength of the composites. Compared with Fig. 10a, it could be found that the phase separation of Fig. 10b was more serious in the larger voids of PLA/PBAT blends, which was the reason for the obvious decrease of flexural strength, tensile strength and notched impact strength of the composites. Poor binding between fiber and matrix and fiber fracture are one of the main reasons for failure of fiber reinforced composites [29]. Compared with Fig. 10a, c and d showed that the voids were obviously reduced and the bonding between the interfaces of composites was closer, which leaded to the increase of tensile and flexural strength of composites. In Fig. 10e, compared with Fig. 10c and d, it could be found that the interface of composite materials improved further the bonding between PLA, PBAT and OWF, which indicated that the mechanical properties of the composites adding two interfacial modifiers of MAPLA and KH560 at the same time were optimal.

Water Absorption Performance Analysis

Water absorption is a significant criterion for many practical applications of natural fiber/PLA products. Figure 11 showed the variation of water absorption of composites with different PBAT content in 1 week. It could be seen that in the first 4 days, the water absorption of the composites increased faster, then the water absorption slowed down. The water absorption of the composite increased stepwise with the increase of PBAT content. The absorbency of the PLA/40PBAT/OWF reached 1.17% on the seventh day. Both PLA and PBAT are hydrophobic materials with little water absorption, and the main components of OWF were cellulose and hemicellulose, which contained a great deal of hydroxyl groups. Therefore, the moisture in the composites was mainly absorbed by lignocellulose fibers. With the increase of PBAT content, the void in the composites increased and the interface was not tightly bonded, which made it easier for the fibers to absorb water, and the water absorption of the composites increased.

Figure 12 presented the variation of water absorption of composites with different interfacial modifier in 1 week. The water absorption of the composites treated with different interfacial modifiers was lower than that of the untreated composites, and the decrease of water absorption of the PLA/20PBAT/OWF composites adding with 2 wt% MAPLA and 2 wt%KH560 at the same time was the most significant. The decrease of water absorption of the PLA/20PBAT/OWF composites adding with 2 wt%KH560 was the second, and the decrease of water absorption of the PLA/20PBAT/OWF composites adding with 2 wt% MAPLA was the least. Since interfacial modifiers reacted with hydroxyl groups in OWF to form chemical bonds, reducing the number of hydroxy groups that absorb water. In addition, the interfacial bonding properties between OWF, PBAT and PLA were improved after the addition of modifier, and the bonding between OWF, PBAT and PLA was closer, thus reducing the contact area between OWF and water and decreasing the water absorption of the composites.

Conclusions

This paper successfully presented the results of a study of thermal and mechanical properties of the environmentally friendly PLA/PBAT/OWF composites. The results demonstrated that the impact toughness of composites was increased significantly with addition of PBAT. From TGA and DSC images, the thermostability of the composites improved with adding PBAT, and the X_c of the composites

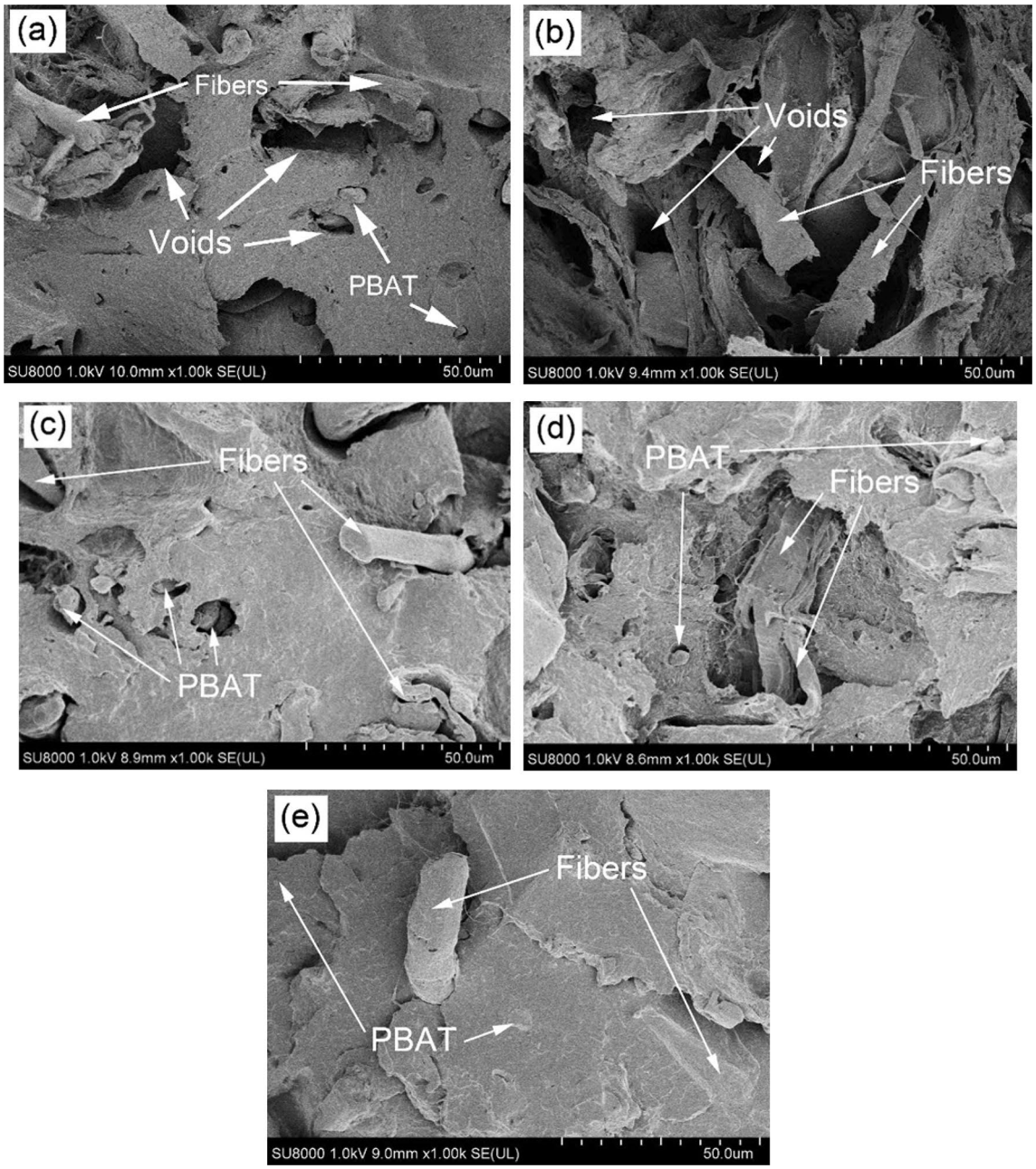

Fig. 10 SEM micrographs of fracture surface of tensile specimen **a** PLA/20PBAT/OWF, **b** PLA/40PBAT/OWF, **c** PLA/20PBAT/OWF/2 M, **d** PLA/20PBAT/OWF/2K and **e** PLA/20PBAT/OWF/MK

improved. However, it could be found that the voids of the composites increased and the interfacial bonding became loose by SEM images. Furthermore, the addition of MAPLA and KH560 increased the mechanical performance of the PLA/PBAT/OWF composites by increasing the interfacial adhesion of OWF, PBAT and PLA. PLA/20PBAT/OWF/MK composites have the optimal stiffness and ductility. To sum up, OWF has a significant enhancement effect on PLA/PBAT composite, making the composite have not bad both tensile strength and flexural strength, and significantly improve impact toughness. The PLA/20PBAT/OWF/MK composites finally prepared have excellent comprehensive properties, which makes the application prospect of PLA more extensive.

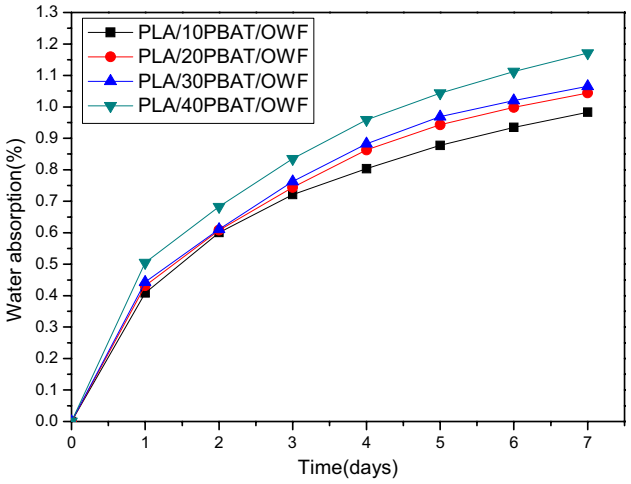

Fig. 11 The variation of water absorption of composites with different PBAT content in 1 week

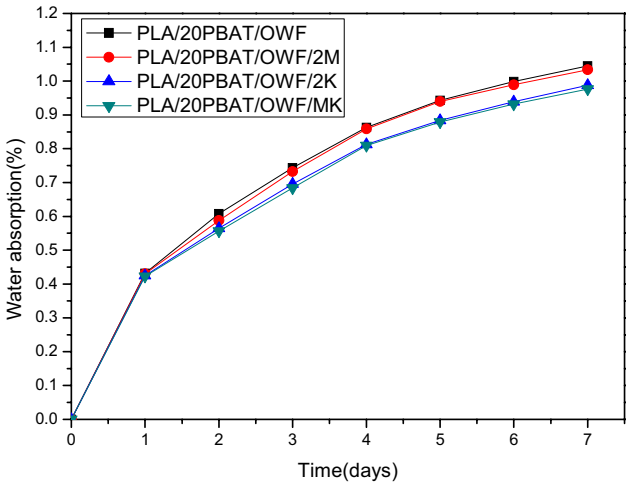

Fig. 12 The variation of water absorption of different interfacial modifier composites in 1 week

Acknowledgements Authors gratefully acknowledge financial supports from Natural Science Foundation of Shaanxi Province (2015JM3080), the Special Research Foundation of Xi'an University of Technology (2014TS008), and the Foundation of Xi'an Beilin District (GX1712).

References

1. Li Y, Xie L, Ma H (2015) Permeability and mechanical properties of plant fiber reinforced hybrid composites. Mater Des 86:313–320
2. Song W, Zhu MH, Zhang SB (2018) Comparison of the properties of fiberboard composites with bamboo green wood, or their combination as the fibrous raw material. BioResources 13:3315–3334
3. Nyambo C, Mohanty AK, Misra M (2010) Polylactide-Based renewable green composites from agricultural residues and their hybrids. Biomacromol 11:1654–1660
4. Ma H, Li Y, Shen YO, Xie L, Wang D (2016) Effect of linear density and yarn structure on the mechanical properties of ramie fiber yarn reinforced composites. Compos Part A 87:98–108
5. Qian S, Sheng K, Yu K, Xu L, Lopez CAF (2018) Improved properties of PLA biocomposites toughened with bamboo cellulose nanowhiskers through silane modification. J Mater Sci 53:10920–10932
6. Jalali A, Huneault MA, Elkoun S (2016) Effect of thermal history on nucleation and crystallization of poly(lactic acid). J Mater Sci 51:7768–7779
7. Yu T, Ren J, Gu SY, Yang M (2010) Preparation and characterization of biodegradable poly(lactic acid)-block-poly(ε-caprolactone) multiblock copolymer. Polym Advan Technol 21:183–188
8. Lu T, Liu S, Jiang M et al (2014) Effects of modifications of bamboo cellulose fibers on the improved mechanical properties of cellulose reinforced poly(lactic acid) composites. Compos Part B 62:191–197
9. Luyt AS, Gasmi S (2016) Influence of blending and blend morphology on the thermal properties and crystallization behaviour of PLA and PCL in PLA/PCL blends. J Mater Sci 51:4670–4681
10. Bai ZF, Dou Q (2018) Rheology, morphology, crystallization behaviors, mechanical and thermal properties of poly(lactic acid)/polypropylene/maleic anhydride-grafted polypropylene blends. J Polym Environ 26:959–969
11. Joffre T, Segerholm K, Persson C, Bardage SL, Hendriks CLL, Isaksson P (2017) Characterization of interfacial stress transfer ability in acetylation-treated wood fibre composites using X-ray microtomography. Ind Crop Prod 95:43–49
12. Jing MF, Che JJ, Xu SM, Liu ZW, Fu Q (2018) The effect of surface modification of glass fiber on the performance of poly(lactic acid) composites: graphene oxide vs. silane coupling agents. Appl Surf Sci 435:1046–1056
13. Zafar MT, Kumar S, Singla RK, Maiti SN, Ghosh AK (2018) Surface treated jute fiber induced foam microstructure development in poly(lactic acid)/jute fiber biocomposites and their biodegradation behavior. Fiber Polym 19:648–659
14. Xu C, Lv Q, Wu D et al (2017) Polylactide/cellulose nanocrystal composites: a comparative study on cold and melt crystallization. Cellulose 24:2163–2175
15. Yeh JT, Tsou CH, Huang CY, Chen KN, Wu CS, Chai WL (2010) Compatible and crystallization properties of poly(lactic acid)/poly(butylene adipate-co-terephthalate) blends. J Appl Polym Sci 116:680–687
16. Wu NJ, Zhang H (2017) Mechanical properties and phase morphology of super-tough PLA/PBAT/EMA-GMA multicomponent blends. Mater Lett 192:17–20
17. Urquijo J, Aranburu N, Dagreou S, Guerrica-Echevarria G, Eguiazabal JI (2017) CNT-induced morphology and its effect on properties in PLA/PBAT-based nanocomposites. Eur Polym J 93:545–555
18. Yu T, Li Y (2014) Influence of poly(butylenes adipate-co-terephthalate) on the properties of the biodegradable composites based on ramie/poly(lactic acid). Compos Part A 58:24–29
19. Faisal A, Salmah H (2012) Mechanical and thermal properties of compatibilized waste office white paper-filled low-density polyethylene composites. J Thermoplast Compos 25:193–207
20. Joshi G, Naithani S, Varshney VK, Bisht SS, Rana V, Gupta PK (2015) Synthesis and characterization of carboxymethyl cellulose from office waste paper: a greener approach towards waste management. Waste Manage 38:33–40
21. Lei WQ, Fang CQ, Zhou X et al (2018) Cellulose nanocrystals obtained from office waste paper and their potential application in PET packing materials. Carbohyd Polym 181:376–385
22. Zhang XL, Bo XF, Wang RM (2013) Study on mechanical properties and water absorption behaviour of wastepaper fibre/recycled polypropylene composites. Polym Polym Compos 21:395–401

23. Serrano A, Espinach FX, Julian F, del Rey R, Mendez JA, Mutje P (2013) Estimation of the interfacial shears strength, orientation factor and mean equivalent intrinsic tensile strength in old newspaper fiber/polypropylene composites. Compos Part B 50:232–238
24. Osman H, Ismail H, Mariatti M (2010) Comparison of reinforcing efficiency between recycled newspaper (RNP)/carbon black (CB) and recycled newspaper (RNP)/silica hybrid filled polypropylene (PP)/natural rubber (NR) composites. J Reinf Plast Comp 29:60–75
25. Qian SP, Sheng KC (2017) PLA toughened by bamboo cellulose nanowhiskers: role of silane compatibilization on the PLA bionanocomposite properties. Compos Sci Technol 148:59–69
26. Chen PY, Lian HY, Shih YF, Chen-Wei SM (2018) Chemically functionalized plant fibers and carbon nanotubes for high compatibility and reinforcement in polylactic acid (PLA) composite. J Polym Environ 26:1962–1968
27. Marais A, Kochumalayil JJ, Nilsson C, Fogelström L, Gamstedt EK (2012) Toward an alternative compatibilizer for PLA/cellulose composites: grafting of xyloglucan with PLA. Carbohyd Polym 89:1038–1043
28. Segal L, Creely JJ, Martin AH, Conrad CM (1959) An empirical method for estimating the degree of crystallinity of native cellulose using the X-ray diffractometer. Text Res J 29:786–794
29. Wang T, Drzal LT (2012) Cellulose-nanofiber-reinforced poly(lactic acid) composites prepared by a water-based approach. Acs Appl Mater Inter 4:5079–5085
30. Reig FB, Adelantado JV, Moya Moreno MCM (2002) FTIR quantitative analysis of calcium carbonate (calcite) and silica (quartz) mixtures using the constant ratio method. Application to Geological samples. Talanta 58:811–821
31. Yaseen SA, Yiseen GA, Li ZJ (2018) Synthesis of calcium carbonate in alkali solution based on graphene oxide and reduced graphene oxide. J Solid State Chem 262:127–134
32. Hopkinson L, Rutt KJ, Kristova P (2018) The near-infrared spectra of the alkali carbonates. Spectrochim Acta A 200:143–149